

GBOT: Graph-Based 3D Object Tracking for Augmented Reality-Assisted Assembly Guidance

Shiyu Li*

Hannah Schieber†

Niklas Corell‡

Bernhard Egger§

Julian Kreimeier¶

Daniel Roth||

Technical University of Munich
School of Medicine and Health
Department Clinical Medicine
Machine Intelligence in Orthopedics
Clinic for Orthopedics and Sports
Orthopedics*,†,¶,||

Human-Centered Computing and
Extended Reality
Friedrich-Alexander-Universität
Erlangen-Nürnberg (FAU)
Erlangen, Germany*,‡,§

Lehrstuhl für Graphische
Datenverarbeitung (LGDV)
Friedrich-Alexander Universität (FAU)
Erlangen-Nürnberg
Erlangen, Germany§

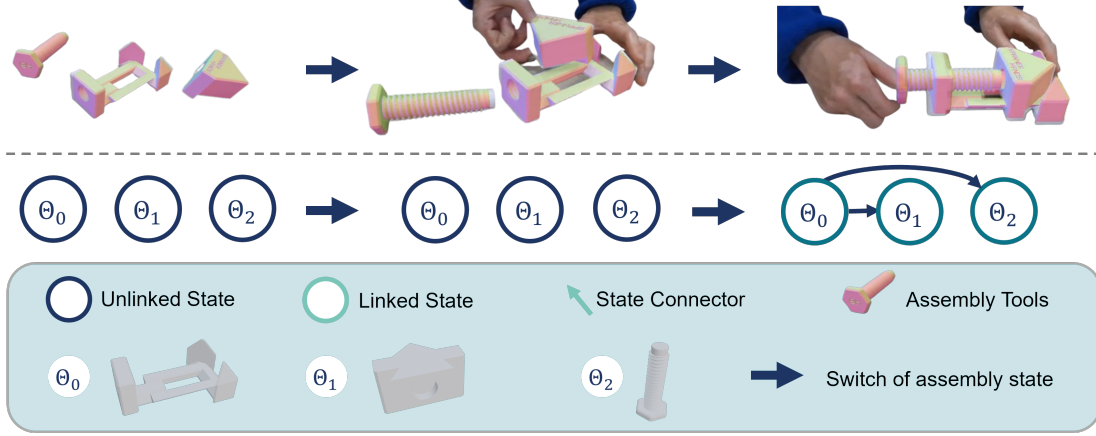


Figure 1: **Our graph-based object tracking algorithm can track objects in their individual assembly states.** We apply kinematic links between objects in different assembly states. For augmented reality based assembly tasks, the assembly state can be automatically detected by the constantly tracked object pose.

ABSTRACT

Guidance for assemblable parts is a promising field for augmented reality. Augmented reality assembly guidance requires 6D object poses of target objects in real time. Especially in time-critical medical or industrial settings, continuous and markerless tracking of individual parts is essential to visualize instructions superimposed on or next to the target object parts. In this regard, occlusions by the user’s hand or other objects and the complexity of different assembly states complicate robust and real-time markerless multi-object tracking. To address this problem, we present Graph-based Object Tracking (GBOT), a novel graph-based single-view RGB-D tracking approach. The real-time markerless multi-object tracking is initialized via 6D pose estimation and updates the graph-based assembly poses. The tracking through various assembly states is achieved by our novel multi-state assembly graph. We update the multi-state assembly graph by utilizing the relative poses of the individual assembly parts. Linking the individual objects in this graph enables more robust object tracking during the assembly process.

*e-mail: shiyu.li@tum.de

†e-mail: hannah.schieber@fau.de

‡e-mail: niklas.corell@fau.de

§e-mail: bernhard.egger@fau.de

¶e-mail: julian.kreimeier@tum.de

||e-mail: daniel.roth@tum.de

**<https://github.com/roth-hex-lab/gbot>

For evaluation, we introduce a synthetic dataset of publicly available and 3D printable assembly assets as a benchmark for future work. Quantitative experiments in synthetic data and further qualitative study in real test data show that GBOT can outperform existing work towards enabling context-aware augmented reality assembly guidance. Dataset and code will be made publically available**.

Index Terms:

Computing methodologies—Artificial intelligence—Computer vision Computing methodologies—Computer graphics—Graphics systems and interfaces—Mixed / augmented reality

1 INTRODUCTION

Accurate and real-time estimation of 6D object pose and robust object tracking play a crucial role in enhancing Augmented Reality (AR) assembly guidance through immersive 3D visualization. This task becomes especially challenging in dynamic scenarios involving multi-object tracking, where assembly states change and occlusions occur [25, 53, 67]. AR-guided assemblies can be widely applied to everyday life [53, 62], industrial settings [8, 16, 40], or in the medical context [25]. Different visualization approaches employing optical or video see-through devices, such as AR head-mounted displays (HMDs) [6, 25] or smartphones [2, 65], have been explored. There is evidence, that AR assembly guidance can outperform pictorial instructions [6, 62], especially in-situ visualizations outperform side-by-side or in-view visualizations [5, 26]. Furthermore, some approaches tackle hand occlusions [65] or authoring instructions [11].

To enable AR-based assembly guidance in medical or industrial settings, real-time markerless tracking is one crucial element. To achieve markerless tracking, the utilization of 6D object pose es-

timization [36, 54, 58, 59] or 6D object tracking [38, 51] is essential. Most deep-learning methods combine object detection or semantic segmentation with a consecutive pose estimation [22, 36, 58]. This consecutive combination can be computationally costly and is often not real-time suitable. 6D object tracking instead is often more efficient but requires an initial pose for each object. Moreover, the focus of tracking or pose estimation is often on a single object [41, 51] instead of multiple objects in various assembly states or requires textured objects [34].

To address this challenge, we present Graph-based Object Tracking (GBOT). A real-time capable graph-based tracking approach enabling multi-object tracking in multi-state assembly tasks. To automatically initialize the tracking prior to the assembly tasks, we harness 6D pose estimation using our YOLOv8Pose. After initialization, the tracking updates the objects' poses constantly. To enable tracking over different assembly steps, we define a graph describing the kinematic links between each assembly pair in different steps. GBOT can dynamically switch between different assembly states while existing graph-based approaches [45, 50] require re-initialization per state. Each assembly step is defined by the relative pose between the objects. If the individual parts are assembled in their relative pose to each other, the linked parts are considered as a module. The tracking of the module is eased by constraining links which regulate the individual objects' Degrees of Freedom (DoF). This enables a more efficient tracking compared to tracking individual assembly parts.

To train and validate our approach, we generated synthetic data of 3D assembly assets. The generated validation data contains scenes with standard (normal) conditions, hand occlusion, dynamic light, and motion blur. To address the sim-to-real gap, we recorded real data without ground truth for qualitative evaluation. Our evaluation compares GBOT with a state-of-the-art tracking approaches [29, 49, 51] and our 6D pose estimation. Our approach shows robustness and real-time capability for object tracking towards AR assembly guidance. In summary, we contribute:

- A real-time multi-object assembly graph tracking driven by 6D pose estimation for multi-state assembly including assembly state identification.
- An annotated synthetic dataset and unlabeled real test data of publicly available and 3D printable assembly assets as a quantitative and qualitative benchmark for AR assembly guidance.

2 RELATED WORK

2.1 Instance-level 6D Pose Estimation

6D object pose estimation predicts the six DoF, namely rotation and translation that define an object's position in a camera coordinate system. Pose estimation can be categorized into two main areas: category-level 6D pose estimation, which involves class-wise pose identification [59, 66] and instance-level 6D pose estimation [3, 18, 64], i.e., identifying the pose for each individual instance of a class.

Instance-level 6D object pose assumes that 3D object models are known during inference. Furthermore, instance-level 6D object pose estimation can be distinguished into one-stage [3, 18, 64] and two-stage [22, 36] approaches. One-stage approaches like PoseCNN [64] or FFB6D [18] rely on semantic segmentation, while SingleShotPose [54] builds upon the object detector YOLO [42]. Using the extracted features, they either regress the pose directly [64], feed extracted points into Perspective-n-Point (PnP) [54] or utilize Least Squares Fitting algorithm [18]. Amini et al. [3] introduce YoloPose which directly regresses keypoints in an image and presents a learnable module to replace PnP.

Moreover, two-stage approaches [36, 58] apply an off-the-shelf object detector and subsequently estimate the 6D pose. These methods restrict real-time capability due to computational cost. Depending

on the choice of the object detection or semantic segmentation backbone, as well as the algorithm employed for 6D pose estimation, one-stage approaches may exhibit greater efficiency, making them better suited for real-time applications.

2.2 Object Tracking

In contrast to 6D pose estimation, object tracking assumes the 6D pose in the initial frame to be known. Object tracking can be divided into region-based [38, 55] and depth-based [4, 10, 12, 14, 21, 37] approaches. Tracking algorithms can suffer from losing track due to heavy occlusion. To address this, DeepIM [28] introduced the re-initialization by PoseCNN [64].

Region-based methods rely on color images to predict the probability that a pixel belongs to the object or to the background based on statistics. PWP3D [38] is the first real-time region-based approach around 20 Hz. 6D object poses are updated based on pixel-wise optimization. Based on this work, Tjaden et al. [55] proposed RBOT, which uses a Gauss-Newton optimization scheme to accelerate the optimization. To make the object tracking more efficient, a sparse tracker SRT3D [49] is introduced using second-order Newton optimization with Tikhonov regularization. Their tracking algorithm reaches about 200 Hz considering occlusion without the need of GPU acceleration.

Depth-based methods use depth cameras to track objects. The most common tracking approach is the Iterative Closest Point (ICP) framework [40, 43]. Other approaches introduce particle filters [12] or Gaussian filters [21].

Besides approaches that only rely on depth or regions, Stoiber et al. [51] propose the hybrid approach ICG. ICG considers visual appearance and adds both region and depth modality on the framework reaching around 788 Hz for a single object. Moreover, Stoiber et al. [48] extend ICG to ICG+ by adding texture modality using visual features like SIFT or ORB. Although this further improves the results, it also extends the computational time. Additionally, Stoiber et al. [50] present a multi-body tracking framework Mb-ICG for kinematic structures. They interpret kinematic structures as graphs and formulate the 6 DoF pose variations of bodies as the vertices of the graph. Their multi-body tracking with kinematic structures considers objects with different regions defined as fixed and movable but is constrained to one object state, which cannot be applied for tracking assembly parts. For tracking initialization, they manually aligned objects to the predefined poses which limits its real AR application with users.

2.3 Datasets for Object Pose and Tracking

To evaluate 6D pose estimation or tracking algorithms, datasets with manifold objects and various scenarios are crucial. LINEMOD [19]/LINEMOD occluded [9] and YCB-Video (YCBV) contain textured objects. T-Less [20] provides texture-less objects which is challenging for feature-based approaches. Most existing datasets [9, 19, 20, 64] contain multiple objects but do not consider dynamic assembly objects with hand occlusion. Therefore, assembly assets with a subset of assembly parts [52, 60] can be considered as a 6D pose estimation dataset for AR-assisted guidance. IKEA-Manual [61] is a assembly dataset with 3D pose of each parts, i.e., rotation of the 3D part but the translation of each parts are not investigated. The IKEA assembly dataset [52] addresses this but is not publicly available. For hand pose estimation, Schoonbeek et al. [46] introduce an assembly dataset. However, it focuses on hand poses instead of object poses.

The RBOT dataset [55] focuses on single object tracking and includes a selection of twelve objects from LINEMOD dataset and five from the Rigid Pose dataset [35]. RBOT is a semi-real dataset with rendered models on real background images. Regarding tracking of kinematic objects, RTB [50] proposed a semi-real dataset with robotic kinematic objects. Another tracking dataset is OPT [63].

It contains single 2D and 3D objects. OPT only contains a single object per frame. In addition, Choi Dataset [13] introduces four kitchen objects and provides RGB-D data both in synthetic scenes with the ground truth object trajectories and real scenes for qualitative evaluation. Moreover, BCOT dataset [27] proposed a marker-less high-precision 3D Object Tracking Benchmark using calibrated binocular cameras and object poses are optimized by the re-projection constraints in all views.

Moreover, the use of synthetic data is common for 6D pose estimation as capturing real-world data is time-consuming and error-prone due to calibration errors. In this regard, Denninger et al. [15] propose Blenderproc, a Blender and python based library to generate synthetic images. Additionally, other tools like Unity or Unreal can also be used to generate synthetic data [7, 33, 39, 44].

2.4 Pose Estimation and Tracking in AR

Utilizing markers [67], object detection [25], pose estimation [53], or tracking [34] enables, for example, the visualization of assembly instructions in AR [25, 67]. Zauner et al. [67] proposed hierarchical structures for authoring AR assembly instructions. To track the objects, visual markers were used. Rambach et al. [41] introduced a 6DoF single object tracking based on 3D Scans for AR.

Moreover, Park et al. [34] proposed a method of multi-object tracking. For object tracking they rely on local features requiring textured objects. Additionally, Wu et al. [62] apply template matching and ICP to track objects in various assembly states. To monitor assembly states they use a tree-like structure, with the closing and combining states which define the connecting components of the assembly parts in a graph. However, their template-based approach is limited in the hand occlusion scenes and with the rise of deep learning, this approach has been outperformed by correspondence-based approaches driven by convolutional neural networks (CNNs). Su et al. [53] proposed a deep-learning-based multi-state object pose estimation for AR assembly tasks, focusing on pose estimation of static objects. Additionally, Kleinbeck et al. [25] utilized synthetic data and deep-learning based object detection to visualize assembly steps. Moreover, Wang et al. [56] proposed a tree-like assembly graph for AR guidance. However, the object detector does not provide the six DoF information for the individual objects and it is not suitable for 3D user interface. Liu et al. [30] train a object detector with an attention module for recognizing objects in multiple scenes. Similarly, Stanescu et al. [47] train a variation of YOLO to identify object in multiple states using a state vector in their object detector.

3 METHODOLOGY

GBOT can be split into two parts: First, 6D object pose estimation is used to initialize the tracking approach. Second, we implement multi-object tracking and identify the assembly states using our multi-state assembly graph. If the tracking is lost, GBOT + re-init, can enable re-initialized again by object pose estimation. The overall framework is depicted in Figure 2. To train and validate our approach we leverage synthetic data generation. Real data is only used for qualitative tests.

3.1 Initial Object Pose Estimation

For our 6D pose estimation, we build upon the state-of-the-art object detector YOLOv8 [23] and due to real-time capability, design it as a one-stager approach [3]. To detect the objects, we extend the detection output to not only bounding boxes but also keypoints for 6D pose estimation [3]. We detect keypoints directly on the objects surfaces instead the corners of 3D bounding boxes [3]. Our architecture is illustrated in Figure 2. The backbone of the YOLOv8 model is CSPDarknet as feature extractor, which is followed by the C2f module. The C2f module feeds to three prediction heads, which learn to predict the object keypoints for the input image. To ensure solid prediction results for small object, we set the input image

size to 1280×720 px. After the keypoints and bounding boxes are detected, they are fed into RANSAC PnP to recover the object pose.

3.1.1 Keypoints Selection

To define surface keypoints on each object, we apply Farthest Point Sampling [3, 36] which initializes a keypoint set on the object surfaces and adds overall N points. In terms of N , three keypoints are the minimum for PnP [32], but this number is not robust with occlusions or symmetric objects limiting the pose estimation. The maximum amount of keypoints used is 24 [3]. Generally, more keypoints slightly improve the accuracy but also increase the computational cost [36]. Due to our varying object sizes, we use 17 as an economic trade-off between keypoint quantity, visibility, and computational time.

3.1.2 6D Pose Prediction

PnP is the problem of solving 6D object pose given a set of N 3D points of object models and corresponding prediction 2D key points. The output of the object detector, i.e., the bounding boxes and keypoints, is processed by RANSAC PnP to recover the 6D object poses. PnP is not robust to outliers if the key points are not accurate. Therefore RANSAC can be applied with PnP to make the pose estimation more reliable. To train the network we apply the loss proposed by YOLOv8 for keypoint regression. [23]:

$$L_{total} = \sum_{i,j,k} (\lambda_{cls} L_{cls} + \lambda_{box} L_{box} + \lambda_{pose} L_{pose} + \lambda_{kobj} L_{kobj} + \lambda_{focal} L_{focal}) \quad (1)$$

where L_{total} represents the total training loss, L_{cls} represents the loss for class labels, L_{pose} represents the key points loss for pose estimation and L_{kobj} represents the keypoint objectiveness loss. Additionally, VariFocal loss [68] L_{focal} is applied [23, 68] considering the overlap of the bounding boxes. $\lambda_{cls} = 0.5$, $\lambda_{box} = 7.5$, $\lambda_{kpts} = 12$, $\lambda_{kobj} = 1.0$, and $\lambda_{focal} = 1.5$ are hyperparameters to balance the loss for the individual tasks, i.e., object detection (class and bounding box), and keypoints.

The pose loss is defined as L2 loss between the predicted value and ground truth value [24, 57].

$$L_{pose} = \|\mathbf{K}_{pred} - \mathbf{K}_{gt}\|_2 \quad (2)$$

where \mathbf{K}_{pred} is the predicted 2D keypoints by deep learning model and \mathbf{K}_{gt} is the ground truth 2D keypoints.

3.2 Graph-based Object Tracking

6D object pose estimation can be used to constantly detect individual objects, but is computationally costly impeding real-time capabilities. Object tracking can provide real-time pose information, but needs a pose for initialization. We use 6D pose estimation for object tracking initialization. A graph-based object tracking is based on updates of object poses at new frames in time [17]. Most of the tracking algorithms (e.g., [50, 55]) define a probabilistic model based on an energy function or a pose variation vector. We use the energy function defined as the negative logarithmic probability following Stoiber et al. [50]. Our tracking in particular extends their graph-based approach [50] which uses kinematic links between different objects to ease the tracking process. In contrast to their work, we update those links in real-time according to the prior known assembly graph. Furthermore, we do not rely on deep learning models detecting assembled parts as new parts [53]. Instead, we specifically consider the spatial combinations of existing objects. Figure 2 shows the structure of our graph-based object tracking pipeline. We use a RGB-D sensor for object detection and tracking providing object poses via a RESTful API. With the API, multiple AR visualization devices can request the object poses.



Figure 4: An overview of all five assembly assets included in the GBOT dataset.



Figure 5: **Our synthetic training images.** Clustered scenes with 3D printing parts for the assembly parts are generated. To add domain randomization, we add objects from the T-less [20] dataset, varying lighting conditions, and randomized backgrounds.

truth translation for two assembly parts.

$$e_{rot} = ||\arccos(\frac{tr(\mathbf{R}_{pred}\mathbf{R}_{gt}^T) - 1}{2})|| \quad (5)$$

where e_{rot} calculates the absolute value of angle offset between predicted rotation matrix \mathbf{R}_{pred} and ground truth \mathbf{R}_{gt} .

Figure 3b shows the procedure for switching between assembly states. As an empirically feasible threshold we chose 3 cm for translation offset and 10 degree for rotation offset.

Before the tracking process begins, object-specific trackers are set for different assembly states. Once an assembly step is detected to be finished, the trackers are automatically switched to the new state. The object poses for pre-assembly parts are used to initialize tracking the assembly as a whole in the next step.

3.3 The GBOT Dataset

Currently, there is no real-world or synthetic dynamic assembly dataset available. We utilized synthetic data to enable an easy extension of the dataset in the future. For real-world scenes, annotating moving poses frame-by-frame as ground truth data is challenging. Synthetic data is a common approach for acquiring ground truth data [44]. To generate training data, we used publicly available 3D models. However, one can also use 3D scans or CAD models. The dataset consists of five 3D printing assembly assets from Thingiverse¹ to test our algorithm, see Figure 4. We used Blender-proc [15] to generate RGB-D data as well as ground truth poses with Azure Kinect intrinsic camera model. To bridge the sim-to-real gap, we apply domain randomization, i.e., varying background textures, different lighting conditions, and distracting objects [44].

To robustly track the object poses during the assembly, we focus on instance-level objects that can be continuously detected. On the one hand, screws and small connectors can be easily occluded by hands and other parts during assembly. On the other hand, there

Table 1: **Objects for evaluation:** The following instances' poses are to be estimated and tracked. Symmetric objects are labelled in **bold**.

Assembly assets	Objects
Hobby Corner Clamp	Clamp Base, Clamp Bolt , Clamp Jaw
Geared Caliper	Fix, Move Bottom, Move Top Vernier
Nano Chuck by PRIma	Balljoint , Base, Headplate , Nut , Screw , Vise base, Vise screw , Vise slider
Hand-Screw Clamp	Jaw 1, Jaw 2, Knob 1 , Knob2 , Pad , Thread 1 , Thread 2
LiftPod	Arm first , Arm last , Bar , Base plate , Clamp frame, Clamp slider, Sleeve

are multiple same screws which lead to only a category-level problem while we focus on the instance-level problem. Therefore, we concentrate on instance-level assembly parts, see Tab. 1.

3.3.1 Training Set

Our training set contains at least 15K images for each assembly asset. The images feature assembled and unassembled objects with 50% of each variant. To improve domain randomization, we generated synthetic data with different textures, scenes and overlays, distracting objects from T-less [20], backgrounds, and varying light conditions, see Figure 5. As ground truth, we export the poses of each object, semantic segmentation mask, and bounding boxes.

3.3.2 Test Set

The test set contains images with 1280×720 px resolution in a total number of $13800 = (900 + 400 + 500 + 750 + 900) * 4$, divided in five assembly sequences. The sequences are normal, different light conditions, motion blur and hand-occlusion, see Figure 6. The normal scene contains objects during the assembly process with an ambient scattered light source. During the sequence, the objects move and get assembled. For capturing, the camera view is fixed and the camera pose is set up to always cover all the assembly parts. The second variant adds dynamic point light based on the first scene. The light point moves randomly in the volume of a sphere to create dynamic light effects. In the third variant blur effects are rendered of moving objects to test the robustness of the tracking algorithm with regard to fast motion. The exposure time is set to one second to capture the blur effects during assembly. For hand occlusion, we use the SMPL human model [15, 31].

Moreover, we record five assembly sequences with Azure Kinect from a top-down view as real test cases. For the real scene, we do not have ground truth poses due to the limitation of annotations. We only use the real scenes for qualitative evaluation.

¹Liftpod, Nano Chuck by PRIma, Hand-Screw Clamp, Hobby Corner Clamp, Geared Caliper

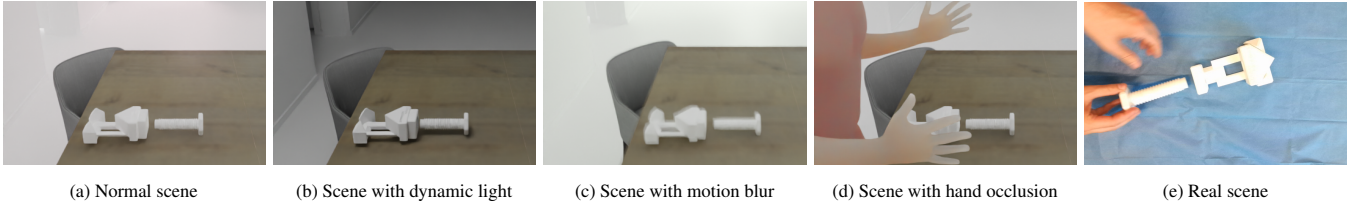


Figure 6: **Synthetic and real scenes with different light conditions, motion blur, and occlusion:** We make ablation studies regarding different light conditions, motion blur, and hand occlusion as real data restrictions.

4 EVALUATION

4.1 Metrics

To evaluate the 6D pose accuracy we follow the state-of-the-art metric Average Distance Error (ADD) [19]. ADD denotes the average distance error e_{ADD} for unsymmetrical objects and $e_{\text{ADD-S}}$ of symmetric objects:

$$e_{\text{ADD}} = \frac{1}{n_v} \sum_{i=1}^{n_v} \|(\mathbf{R}_{\text{pred}} \mathbf{x}_i + \mathbf{T}_{\text{pred}}) - (\mathbf{R}_{\text{gt}} \mathbf{x}_i + \mathbf{T}_{\text{gt}})\|, \quad (6)$$

$$e_{\text{ADD-S}} = \frac{1}{n_v} \sum_{i=1}^{n_v} \min_{j \in [n_v]} \|(\mathbf{R}_{\text{pred}} \mathbf{x}_i + \mathbf{T}_{\text{pred}}) - (\mathbf{R}_{\text{gt}} \mathbf{x}_j + \mathbf{T}_{\text{gt}})\| \quad (7)$$

where e_{ADD} represents the average distance between predicted model points and ground truth model points, \mathbf{x} is a vertex point from the 3D object mesh written in object coordinates, n_v is the number of vertices of object mesh, the average distance $e_{\text{ADD-S}}$ for symmetric objects is computed using the closest point distance between \mathbf{x}_i and \mathbf{x}_j .

The 6D pose is considered to be correct if the average distance is smaller than a predefined threshold. ADD/ADD-S are computed based on the formula below:

$$s_i = \frac{1}{n_f} \sum_{j=1}^{n_f} \max \left(1 - \frac{e_j}{e_t}, 0 \right), \quad (8)$$

with $s_i \in \text{ADD, ADD-S}$, n_f the number of frames, and e_t an error threshold which is defined as 10 cm in our case.

However, these metrics cannot measure the translation and rotation error intuitively. Especially in the use case of AR, the error measured in length and angle need to be defined for our assembly state acquirement, so we defined the metrics as follows:

$$e_{\text{ave_trans}} = \frac{1}{n_f} \sum_{i=1}^{n_f} \|\mathbf{t}_{\text{pred}} - \mathbf{t}_{\text{gt}}\| \quad (9)$$

$$e_{\text{ave_rot}} = \frac{1}{n_f} \sum_{i=1}^{n_f} \left\| \arccos \left(\frac{\text{tr}(\mathbf{R}_{\text{pred}} \mathbf{R}_{\text{gt}}^T) - 1}{2} \right) \right\| \quad (10)$$

where $e_{\text{ave_trans}}$ is the translation error measured in cm and $e_{\text{ave_rot}}$ is the rotation error measured in degree. \mathbf{R}_{gt} denotes the ground truth rotation and \mathbf{t}_{gt} the ground truth translation. \mathbf{R}_{pred} describes the predicted rotation and \mathbf{t}_{pred} the predicted rotation.

Additionally, we report the average inference runtime measured in ms for each algorithm.

4.2 Implementation Details

Our object pose estimation algorithm extends YOLOv8 [23], is implemented in PyTorch for 6D pose estimation, and uses NVIDIA TensorRT to accelerate and optimize inference performance. YOLOv8Pose inference engine, our tracking, and the RESTful API are implemented in C++ 17. For the RESTful API we use

Table 2: **Average runtime in ms of the compared methods.**

Approach	Avg. runtime [ms]
6D pose estimation	
YOLOv8Pose (ours)	63.60
Tracking	
SRT3D [49]	11.87
ICG [51]	27.75
ICG+SRT3D [29, 49, 51]	38.75
GBOT (ours)	28.32
6D pose estimation + Tracking	
GBOT + re-init (ours)	36.89

Restbed [1]. Via our RESTful API, individual output devices can access our tracking data. The code of GBOT is publicly available on GitHub to ensure reproducibility and reusability for further future study.

We use a workstation with an Intel(R) Core(TM) i9-10980XE CPU and NVIDIA GeForce RTX 3090 GPU with 24GB VRAM. For GBOT we additionally followed the implementation of a re-initialization, denoted as GBOT + re-init in the following. We added re-initialization every 10th frame [28] if the tracking offset is larger than 5cm compared with YOLOv8Pose.

4.3 Evaluation on GBOT Dataset

For evaluation we used the test split our GBOT dataset with four conditions (normal, dynamic light, motion blur, hand occlusion). We compare our YOLO-based 6D pose estimation, denoted as YOLOv8Pose, the state-of-the-art tracking approaches [49, 51] and our multi-state assembly tracking approach GBOT. We do not compare our approach with Mb-ICG [50], because it needs a re-initialization per assembly step. Mb-ICG is a single-state approach, which cannot be applied to the multi-state assembly sequences. For YOLOv8Pose we conducted two training strategies. First, we trained it only on unassembled objects and evaluated its performance. Then, we trained YOLOv8Pose on the full training split including assembled objects. We evaluate the performance separately for assembled assets of Hobby Corner Clamp, Geared Caliper, Nano Chuck by PRiMa, Hand-Screw Clamp and Liftpod, see Table 1.

4.4 Quantitative Evaluation

The evaluation of the four different conditions of the GBOT dataset in Table 3 shows that the overall accuracy of the tracking approaches is higher compared to the deep learning-based approach.

The first assembly asset includes three assembly parts. The more parts an asset has, the more challenging the tracking is, see Table 3. For the Hobby Corner Clamp with three parts, GBOT achieves 100.0 for ADD/ADD-S in three conditions. The average translation error was in the best case 0.6 cm and the rotation error was smaller than 3°. The last two assembly assets have more complex assembly parts

Table 3: **Results on the GBOT dataset:** Rotational errors are only evaluated for unsymmetrical objects. We report ADD(S) (\uparrow) with 10cm threshold, the translation error in centimeters (cm) (e_{ave_trans} denoted as e_{trans} , \downarrow) and the rotation error (e_{ave_rot} denoted as e_{rot} , \downarrow) in degrees. The best results among all methods are labeled in bold. In this evaluation, tracking is initialized with ground truth pose only for the first frame and the pose is not reinitialized afterwards. In the last column, we show the tracking results of tracking re-initialization by pose estimation. GBOT outperforms the state-of-the-art tracking approaches, GBOT re-init and YOLOv8Pose.

Approach		6D pose estimation									Tracking												6D pose estimation + tracking		
Modality		RGB									RGB-D														
Asset	Condition	YOLOv8Pose (ours, without assembly)			YOLOv8Pose (ours, with assembly)			SRT3D [49]			ICG [51]			ICG+SRT3D [29,49,51]			GBOT (ours)			GBOT + re-init (ours)					
		ADD(S)↑	e_{trans} ↓	e_{rot} ↓	ADD(S)↑	e_{trans} ↓	e_{rot} ↓	ADD(S)↑	e_{trans} ↓	e_{rot} ↓	ADD(S)↑	e_{trans} ↓	e_{rot} ↓	ADD(S)↑	e_{trans} ↓	e_{rot} ↓	ADD(S)↑	e_{trans} ↓	e_{rot} ↓	ADD(S)↑	e_{trans} ↓	e_{rot} ↓			
Hobby Corner Clamp	Normal	50.2	17.0	38.9	91.5	9.3	3.8	89.8	4.7	25.8	100.0	0.1	38.7	100.0	1.3	38.7	100.0	0.6	2.1	99.5	0.7	2.7			
	Dynamic	56.7	18.0	37.4	99.0	2.5	4.8	88.4	3.7	25.0	100.0	1.5	46.8	100.0	2.0	47.8	100.0	0.6	23.2	100.0	0.5	3.5			
	Hand	18.3	31.6	133.5	45.4	54.1	97.1	66.6	8.8	37.1	68.4	7.4	59.4	68.4	7.5	58.3	81.9	5.7	90.4	90.6	4.4	84.7			
	Blur	50.4	18.0	38.1	97.3	4.0	4.3	88.9	5.0	30.4	100.0	0.5	2.2	100.0	1.0	3.0	100.0	0.6	2.1	99.9	0.6	2.1			
Geared Caliper	Normal	99.3	2.3	42.0	99.6	1.4	10.1	90.6	1.8	5.4	100.0	0.2	2.6	100.0	0.3	3.0	100.0	0.2	2.1	100.0	0.5	3.3			
	Dynamic	93.3	3.8	41.0	99.9	1.3	9.3	92.7	1.4	9.9	100.0	0.2	2.5	100.0	0.4	3.6	100.0	0.2	2.3	100.0	0.5	3.6			
	Hand	98.2	2.7	38.8	99.2	2.4	12.5	96.5	0.9	4.4	85.4	3.0	30.0	85.5	3.1	30.0	85.4	3.0	30.0	99.6	0.8	7.0			
	Blur	99.1	2.2	39.4	99.6	1.4	9.9	98.9	0.9	8.7	100.0	0.2	2.5	100.0	0.3	2.8	100.0	0.2	2.2	100.0	0.5	3.6			
Nano Chuck by PRIma	Normal	19.6	19.6	139.0	71.1	8.8	4.8	74.1	6.6	13.8	89.8	2.1	16.7	89.4	2.3	16.5	99.8	0.6	7.2	93.8	2.4	3.6			
	Dynamic	18.5	26.4	144.8	72.6	7.6	4.6	63.4	10.3	15.6	87.3	3.9	15.3	87.3	4.1	15.8	96.0	2.4	20.0	92.9	2.5	3.7			
	Hand	17.7	30.1	120.7	65.9	11.0	4.7	61.4	13.6	15.3	76.5	6.0	18.3	75.8	6.1	18.1	72.9	8.7	14.5	87.8	3.1	7.3			
	Blur	19.7	20.4	150.6	70.9	9.9	5.2	61.9	11.6	15.2	91.6	1.9	11.4	91.5	2.1	11.1	95.7	0.7	25.1	92.7	3.0	4.7			
Hand- Screw Clamp	Normal	45.8	17.3	66.4	73.5	7.7	17.6	86.5	4.7	8.9	96.0	1.2	1.1	95.9	1.4	2.3	98.8	0.4	0.9	83.7	3.0	4.7			
	Dynamic	38.1	17.5	64.8	82.0	6.7	18.4	86.4	5.6	27.0	95.9	1.7	2.1	95.9	2.2	3.4	98.8	0.6	1.7	91.6	2.1	6.1			
	Hand	33.4	18.7	80.9	67.2	14.2	39.8	60.1	14.3	37.7	73.4	6.9	53.4	73.1	7.1	53.4	68.7	7.9	61.9	83.9	4.9	27.2			
	Blur	44.3	16.7	66.1	85.6	6.5	18.6	86.5	5.6	34.6	95.7	3.0	6.6	95.7	3.2	7.7	98.6	1.2	1.1	91.1	3.0	4.8			
LiftPod	Normal	26.9	24.3	119.6	69.1	13.4	6.7	68.9	11.5	60.0	100.0	0.3	2.3	100.0	0.7	3.9	100.0	0.2	1.5	84.3	5.5	11.4			
	Dynamic	28.4	26.8	127.8	64.3	11.6	7.7	56.0	14.4	6.8	85.1	7.7	42.9	85.0	8.1	45.4	100.0	0.3	1.6	80.8	5.5	13.1			
	Hand	25.6	29.3	116.7	62.6	19.6	19.9	39.1	25.6	60.6	51.7	17.6	74.9	51.8	17.8	76.8	51.7	17.6	74.9	70.0	10.1	7.2			
	Blur	31.1	24.3	123.7	68.3	13.9	6.9	76.9	11.9	5.2	100.0	0.3	2.9	100.0	0.8	3.4	100.0	0.2	1.4	83.1	5.7	10.3			
Mean	Overall	45.7	18.4	86.5	79.2	10.4	15.3	76.7	8.1	22.4	89.8	3.3	21.6	89.8	3.6	22.3	92.4	2.6	18.3	91.3	3.0	10.7			

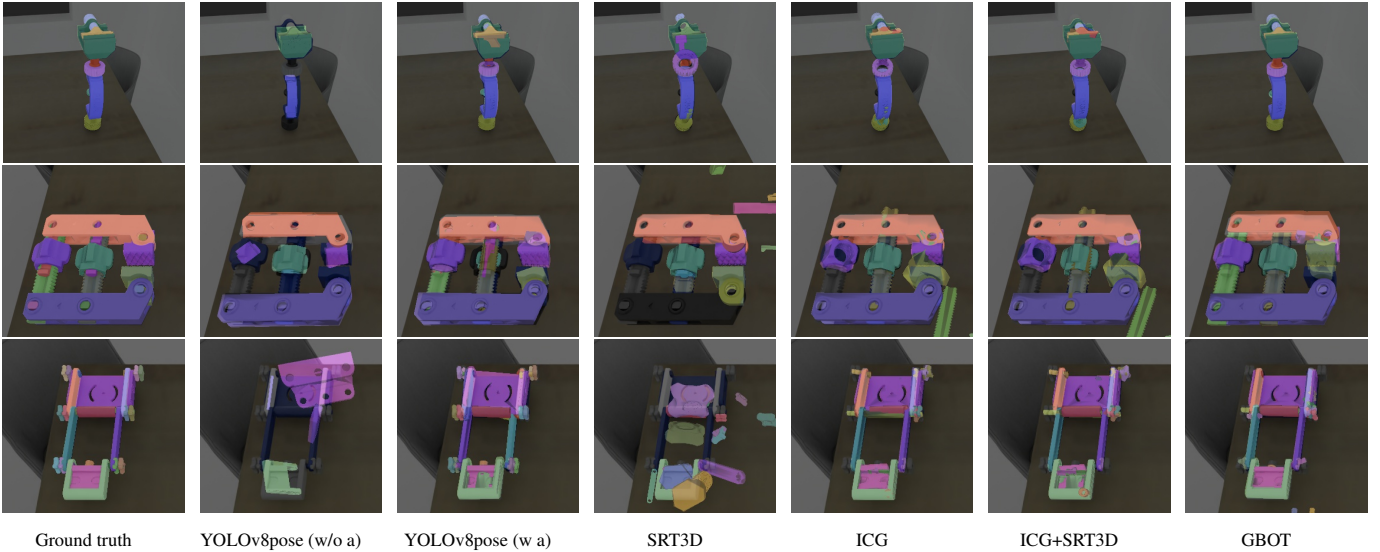


Figure 7: **Qualitative evaluation on the GBOT synthetic dataset.** We compared on the three assembly tools, Nano Chuck by Prima, Hand-Screw Clamp, and Liftpod (top to bottom). Tracked objects are colored individually. It becomes apparent that with a progressing assembly state, GBOT is more aware of the tracking than the state-of-art trackers.

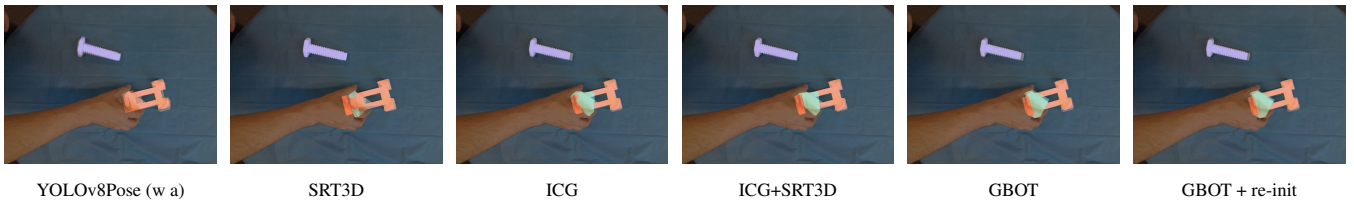


Figure 8: **Qualitative evaluation of GBOT compared to YOLOv8Pose, SRT3D, ICG, ICG+SRT3D and GBOT + re-init on a real scene.** We compared the assembly tool Hobby Corner Clamp with on the different methods. We show the tracked objects in individual colors. YOLOv8Pose cannot detect and estimate the pose of occluded assembly objects, while the tracking algorithm is still able to update object poses. It becomes apparent that with a progressing assembly state, GBOT is more aware of the tracking than the state-of-art trackers SRT3D, ICG and ICG+SRT3D.

than the first asset. Objects like bars or arms contain geometric ambiguity in some special views.

The quantitative results show that GBOT outperforms SRT3D, ICG and ICG+SRT3D. Different from the results on a single-state dataset [29, 64], our experiment shows that ICG+SRT3D [29] does not outperform ICG when using multi-state assembly data. We achieved higher ADD/ADD-S values of 92.4, lower translation error of 2.6 cm and rotation error of 18.3° on average. GBOT + re-init, updates the tracking regularly by 6D pose estimation, has the accuracy between YOLOv8Pose and GBOT in synthetic data, with ADD/ADD-S values of 91.3. We can observe beneficial results on occluded scenes as indicated by the evaluation on the hand conditions for all assembly objects. On real-scenes we also observed that objects which suffer from heavy occlusion during the assembly can benefit from the re-initialization, see Figure 13.

Regarding the runtime, our YOLOv8Pose is about 35 ms slower than our object tracking, see Table 2. SRT3D is the fastest algorithm with 11.87 ms in average considering only RGB tracking. ICG is 15.88 ms slower than SRT3D due to introduction of depth modality. ICG+SRT3D takes extra 11 ms for pose refinement. The latency of our GBOT is about 0.57 ms larger than the state of art object detector ICG. GBOT + re-init, takes overall 36.89 ms per frame. It needs less than 3 ms for one single object. Overall, GBOT and the extension GBOT + re-init are both suitable for real-time applications.

4.5 Qualitative Evaluation

To compare our approach with state-of-the-art tracking approaches, we used the metric-based comparison in Table 1 and compared qualitatively on synthetic and real scenes. We show the results on the synthetic scenes in Figure 7. Qualitative results on the real-3D printing parts are shown in Figure 13 and Figure 8. Figure 7 shows characteristic visualizations of the tracking for the three assembly assets. As shown in Figure 7, GBOT is more robust compared with YOLOv8Pose and common tracking approaches. GBOT can especially track smaller parts. These parts are not lost during the assembly process based on the links to the frame parts. In the case of strong hand occlusion, the tracking suffers when the tracked object is highly occluded by a hand.

The tracking benefits from re-initialization in heavy occluded scenes, see Table 3 and Figure 13. Although our tracking approach works well with assembly assets, GBOT can also have fail cases. We show a qualitative breaking analysis in Figure 13.

4.6 Real Scenes

Besides evaluating on synthetic scenes, we perform additional experiments on real data to show the effectiveness of our approach.

Cluttered scenes with YOLOv8pose: In each cluttered scene we select one assembly asset from the GBOT dataset and other 3D printing parts and randomly place them on a table. We find our YOLOv8pose can still robustly detect objects in clustered scenes, as shown in Figure 9.

Effect of assembly training data: To validate the positive effects of assembly-aware training, we evaluate YOLOv8pose with and without assembly training, see Table 3. Figure 10 shows the qualitative comparison using training data with and without assembly assets. This can explain the improvement in Table 3. Compared with training of separate parts, training data with assembly parts can enhance the detection performance. Assembly assets usually include self-occlusion of separate parts. Considering assembled objects helps to reduce the domain gap between synthetic training data and real test data.

Effect of assembly-state-graph on tracking: In Figure 11, we study the qualitative results of tracking with and without assembly graph. Using assembly constraints, the combined tracking is more accurate than separate tracking. This qualitative comparison is in accordance with the quantitative results in Table 3. Tracking

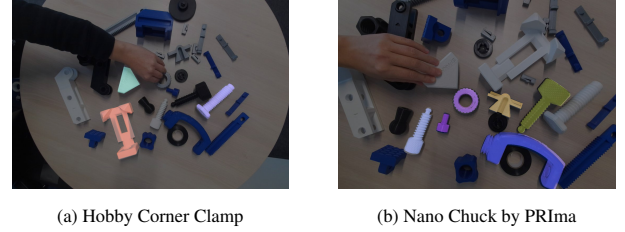


Figure 9: **Evaluation on real cluttered scenes:** We randomly place GBOT assembly assets together with some distract objects to test the influence of cluttered scenes. Our training data with domain randomization helps to detect objects in the cluttered scenes.

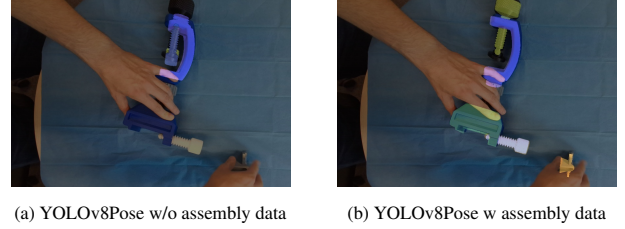


Figure 10: **Assembly-aware training on synthetic scenes and evaluation on a real scene:** Our training data with assembly data helps to overcome occlusion during the assembly process.



Figure 11: **Tracking with assembly-state-graph in a real scene:** We extend our assembly-aware tracking based on work of MbICG [50]. The introduction of assembly state graph helps improve tracking accuracy considering assembly constraints.

with assembly constraints is more robust due to prior knowledge of relative poses between parts. If one of the separate tracking is lost, it can still be recovered from poses of other parts.

4.7 Augmented Reality Integration

GBOT is able to be deployed in real-time to ensure its use in AR applications. To prove this, we show an AR application assembly guidance example of 3D printing parts from the GBOT dataset. As shown in Figure 12, GBOT enables AR HMDs to visualize tooltips or overlays on real objects. Currently, we provide a client-server architecture to handle computational costly tracking on the server side and lightweight AR visualization on the client side. The GBOT framework contains a RESTful API, to request the captured poses of our tracked objects by mobile devices. This pipeline can be utilized to visualize assembly instructions and guidance, as shown in Figure 12. For the current demo we used a Microsoft Hololens 2.

5 DISCUSSION

GBOT utilizes a deep learning-based 6D pose estimation to initialize the tracking. It shows more robust results compared to purely deep-learning based 6D pose estimation and the state-of-the-art tracking.

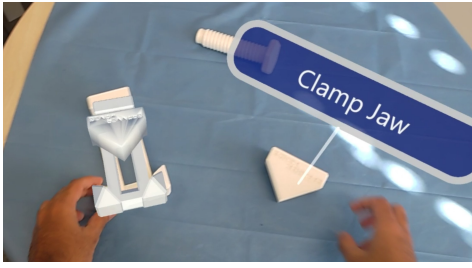


Figure 12: **Augmented reality integration:** Our GBOT tracking algorithm is able to feed a HMD with 6D object pose information, enabling realtime visualization overlays or tooltips on real assembly parts.

Our evaluation shows that pose estimation without assembly training data only works well at the beginning of tracking without assembly occlusion, but fails during the assembly process. With more context-aware training data, the performance of YOLOv8Pose in an assembly scene can be improved. Nevertheless, GBOT has more accurate results compared to YOLOv8Pose. This can be explained by the occlusion during the assembly process and the objects are difficult to be detected during each assembly step. However, the tracking utilizes the information from previous timestamps. With ongoing assembly states, as visualized in our quantitative results, the tracking works more robustly. Including the links between the individual objects showed better results than using an individual tracking like ICG [51].

Generally, tracking smaller objects is difficult. Our strategy is to focus on the main assembly parts, the frame and base parts of the assembly objects and then link smaller objects to the frame parts according to the new assembly state information. This approach helps to overcome losing the tracking during the assembly process. Another important influence factor is the hand occlusion and dynamic light conditions. There are some fail cases, when the tracking is lost during the process and the assembly state cannot be switched to the next step. When the objects are fully occluded by hands or light condition changes swiftly, the tracking suffers. This can be supported by the re-initialization. As shown in Table 1, with occlusion (hand), the re-initialization is beneficial.

Nevertheless, GBOT performs well in tracking assembly parts and we outperform the individual tracking (ICG) on the GBOT dataset. Although the performance in situations of hand occlusion, dynamic light and motion blur is lower than in the normal scene condition, the tracking is still more robust compared to the state-of-the-art. Especially, when looking at qualitative results on synthetic and real scenes, the robustness of our tracking becomes apparent.

5.1 Limitations

In terms of deep learning-driven keypoint detection, symmetric objects are particular challenging. At the same time, smaller objects are challenging for object detectors like YOLO. With deeper convolutions, the smaller parts are at some point not anymore a part of the produced feature map of the network. Moreover, for our YOLO-based approach, we found limitations in occluded scenarios and dynamic light settings. In occluded scenes a re-initialization can be beneficial as indicated by our ablation study using GBOT + re-init. We implement re-initialization following the state-of-the-art approach [28], but the results show limitations in non-occluded scenes with less accuracy.

6 FUTURE WORK

Our approach focuses on textureless printing parts. Future challenges could contain reflective or transparent objects like medical

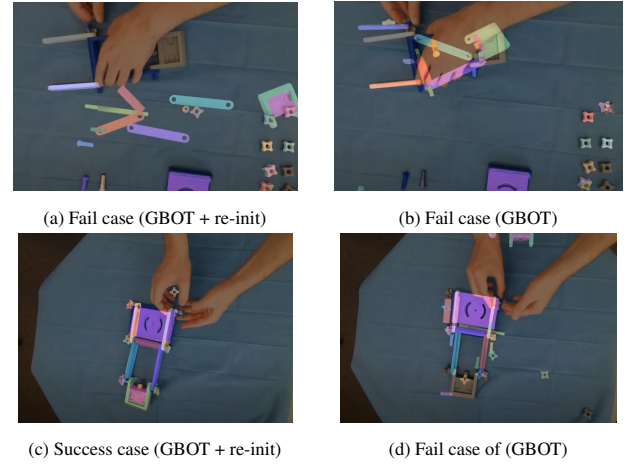


Figure 13: **Possible fail cases of GBOT due to hand occlusion during real assembly process.** Our tracking approach has significant improvement compared to the state-of-art approach. However, after heavy occlusion (top), the tracking without re-initialization suffers.

instruments to further test the boundaries of the tracking approach. Improving our 6D pose estimation algorithm with geometric priors could address robustly tracking target smaller objects with geometric ambiguities. Also, screws or similar objects could be detected more on a category-level basis to enable a more scalable approach for connecting parts of the individual assembly assets. To overcome occlusions, a multi camera setup could be useful, possibly also including AR devices' cameras. To address more challenging assembly objects, a more robust tracking re-initialization might be necessary.

7 CONCLUSION

In this paper, we proposed a novel real-time capable graph-based tracking approach for AR-assisted assembly tasks. GBOT tracks multiple assembly parts using kinematic links based on prior knowledge of assembly poses and combines the knowledge of 6D pose estimation with object tracking. Our tracking enables GBOT to continuously track the objects during the assembly processes in various conditions. To enable a comparison with the state-of-the-art in various scenarios, we propose the synthetic GBOT dataset and extra recorded real scenes. On this dataset, we evaluate our YOLOv8Pose, the tracking approaches SRT3D, ICG, ICG+SRT3D and GBOT. Our dataset contains five assembly assets each with three or more individual parts. The scenes of the datasets have four conditions, normal, dynamic light, motion blur, and hand occlusion. GBOT performs well in synthetic scenes with different lighting, hand occlusions and fast movement as well as real-recorded scenes. We show that tracking is more accurate compared to YOLOv8Pose and that using our dynamically created kinematic links is superior compared to individual tracking. GBOT outperforms the state-of-art tracking algorithms on the GBOT dataset which is easy to reproduce and aims as benchmark for assembly tasks. In conclusion, our approach and dataset are a promising step towards real-time and robust object tracking with AR-guided assembly processes.

ACKNOWLEDGMENTS

The authors thank Philipp Stefan, Patrick Wucherer, and Matthew Lau from Medability GmbH for providing the 3D printed assembly parts. This work is funded by The German Federal Ministry of Education and Research (BMBF) with grant number 16SV8973.

REFERENCES

- [1] Restbed. <https://github.com/Corvusoft/restbed>.
- [2] J. Alves, B. Marques, M. Oliveira, T. Araújo, P. Dias, and B. S. Santos. Comparing spatial and mobile augmented reality for guiding assembling procedures with task validation. In *2019 IEEE International Conference on Autonomous Robot Systems and Competitions (ICARSC)*, pp. 1–6. doi: 10.1109/ICARSC.2019.8733642
- [3] A. Amini, A. Selvam Periyasamy, and S. Behnke. YOLOPose: Transformer-based multi-object 6d pose estimation using keypoint regression. In *Intelligent Autonomous Systems 17: Proceedings of the 17th International Conference IAS-17*, pp. 392–406. Springer, 2023.
- [4] P. Besl and N. D. McKay. A method for registration of 3-d shapes. *IEEE Transactions on Pattern Analysis and Machine Intelligence*, 14(2):239–256, 1992. doi: 10.1109/34.121791
- [5] J. Blattgerste, P. Renner, B. Streng, and T. Pfeiffer. In-Situ Instructions Exceed Side-by-Side Instructions in Augmented Reality Assisted Assembly. In *Proceedings of the 11th Pervasive Technologies Related to Assistive Environments Conference*, pp. 133–140. ACM, Corfu Greece, June 2018. doi: 10.1145/3197768.3197778
- [6] J. Blattgerste, B. Streng, P. Renner, T. Pfeiffer, and K. Essig. Comparing Conventional and Augmented Reality Instructions for Manual Assembly Tasks. In *Proceedings of the 10th International Conference on Pervasive Technologies Related to Assistive Environments, PETRA '17*, pp. 75–82. Association for Computing Machinery, New York, NY, USA, June 2017. doi: 10.1145/3056540.3056547
- [7] S. Borkman, A. Crespi, S. Dhakal, S. Ganguly, J. Hogins, Y.-C. Jhang, M. Kamalzadeh, B. Li, S. Leal, P. Parisi, C. Romero, W. Smith, A. Thaman, S. Warren, and N. Yadav. Unity perception: Generate synthetic data for computer vision, 2021.
- [8] E. Bottani and G. Vignali. Augmented reality technology in the manufacturing industry: A review of the last decade. 51(3):284–310, 2019. doi: 10.1080/24725854.2018.1493244
- [9] E. Brachmann, A. Krull, F. Michel, S. Gumhold, J. Shotton, and C. Rother. Learning 6d object pose estimation using 3d object coordinates. In *Computer Vision—ECCV 2014: 13th European Conference, Zurich, Switzerland, September 6–12, 2014, Proceedings, Part II 13*, pp. 536–551. Springer, 2014.
- [10] Y. Chen and G. Medioni. Object modelling by registration of multiple range images. *Image and vision computing*, 10(3):145–155, 1992.
- [11] S. Chidambaram, H. Huang, F. He, X. Qian, A. M. Villanueva, T. S. Redick, W. Stuerzlinger, and K. Ramani. ProcessAR: An augmented reality-based tool to create in-situ procedural 2D/3D AR Instructions. In *Designing Interactive Systems Conference 2021, DIS '21*, pp. 234–249. Association for Computing Machinery, New York, NY, USA, June 2021. doi: 10.1145/3461778.3462126
- [12] C. Choi and H. I. Christensen. RGB-d object tracking: A particle filter approach on GPU. In *2013 IEEE/RSJ International Conference on Intelligent Robots and Systems*, pp. 1084–1091. IEEE, 2013.
- [13] C. Choi and H. I. Christensen. Rgb-d object tracking: A particle filter approach on gpu. In *2013 IEEE/RSJ International Conference on Intelligent Robots and Systems*, pp. 1084–1091. IEEE, 2013.
- [14] A. I. Comport, E. Marchand, M. Pressigout, and F. Chaumette. Real-time markerless tracking for augmented reality: the virtual visual servoing framework. 12(4):615–628, 2006.
- [15] M. Denninger, M. Sundermeyer, D. Winkelbauer, D. Olefir, T. Hodan, Y. Zidan, M. Elbadrawy, M. Knauer, H. Katam, and A. Lodhi. BlenderProc: Reducing the reality gap with photorealistic rendering. 2020.
- [16] M. Eswaran, A. K. Gulivindala, A. K. Inkulu, and M. V. A. R. Bahubalendruni. Augmented reality-based guidance in product assembly and maintenance/repair perspective: A state of the art review on challenges and opportunities. *Expert Systems with Applications*, 2023.
- [17] Z. Fan, Y. Zhu, Y. He, Q. Sun, H. Liu, and J. He. Deep learning on monocular object pose detection and tracking: A comprehensive overview. *ACM Computing Surveys*, 55(4):1–40, 2022.
- [18] Y. He, H. Haibin, F. Haoqiang, C. Qifeng, and S. Jian. Ffb6d: A full flow bidirectional fusion network for 6d pose estimation. In *IEEE/CVF Conference on Computer Vision and Pattern Recognition*, 2021.
- [19] S. Hinterstoisser, V. Lepetit, S. Ilic, S. Holzer, G. Bradski, K. Konolige, and N. Navab. Model based training, detection and pose estimation of texture-less 3d objects in heavily cluttered scenes. In *Computer Vision—ACCV 2012: 11th Asian Conference on Computer Vision, Daejeon, Korea, November 5–9, 2012, Revised Selected Papers, Part I 11*, pp. 548–562. Springer, 2013.
- [20] T. Hodan, P. Haluza, S. Obdrzalek, J. Matas, M. Lourakis, and X. Zabulis. T-LESS: An RGB-d dataset for 6d pose estimation of texture-less objects. *IEEE Winter Conference on Applications of Computer Vision (WACV)*, 2017.
- [21] J. Issac, M. Wüthrich, C. G. Cifuentes, J. Bohg, S. Trimpe, and S. Schaal. Depth-based object tracking using a robust gaussian filter. In *2016 IEEE International Conference on Robotics and Automation (ICRA)*, pp. 608–615. IEEE, 2016.
- [22] T. Jantos, M. Hamdad, W. Granig, S. Weiss, and J. Steinbrener. PoET: Pose estimation transformer for single-view, multi-object 6d pose estimation. In *6th Annual Conference on Robot Learning (CoRL 2022)*, 2022.
- [23] G. Jocher, A. Chaurasia, and J. Qiu. YOLO by ultralytics. <https://github.com/ultralytics/ultralytics>, 2023.
- [24] A. Kendall and R. Cipolla. Geometric loss functions for camera pose regression with deep learning. In *Proceedings of the IEEE conference on computer vision and pattern recognition*, pp. 5974–5983.
- [25] C. Kleinbeck, H. Schieber, S. Address, C. Krautz, and D. Roth. ARTFM: Augmented reality visualization of tool functionality manuals in operating rooms. In *2022 IEEE Conference on Virtual Reality and 3D User Interfaces Abstracts and Workshops (VRW)*, pp. 736–737. IEEE, 2022.
- [26] E. Laviola, M. Gattullo, A. Evangelista, M. Fiorentino, and A. E. Uva. In-situ or side-by-side? A user study on augmented reality maintenance instructions in blind areas. *Computers in Industry*, 144:103795, Jan. 2023. doi: 10.1016/j.compind.2022.103795
- [27] J. Li, B. Wang, S. Zhu, X. Cao, F. Zhong, W. Chen, T. Li, J. Gu, and X. Qin. Bcot: A markerless high-precision 3d object tracking benchmark. In *Proceedings of the IEEE/CVF Conference on Computer Vision and Pattern Recognition*, pp. 6697–6706, 2022.
- [28] Y. Li, G. Wang, X. Ji, Y. Xiang, and D. Fox. Deepim: Deep iterative matching for 6d pose estimation. In *Proceedings of the European Conference on Computer Vision (ECCV)*, pp. 683–698, 2018.
- [29] Y. Li, F. Zhong, X. Wang, S. Song, J. Li, X. Qin, and C. Tu. For a more comprehensive evaluation of 6dof object pose tracking. *arXiv preprint arXiv:2309.07796*, 2023.
- [30] H. Liu, Y. Su, J. Rambach, A. Pagani, and D. Stricker. Tga: Two-level group attention for assembly state detection. In *2020 IEEE International Symposium on Mixed and Augmented Reality Adjunct (ISMAR-Adjunct)*, pp. 258–263. IEEE, 2020.
- [31] M. Loper, N. Mahmood, J. Romero, G. Pons-Moll, and M. J. Black. SMPL: A skinned multi-person linear model. *ACM Trans. Graphics (Proc. SIGGRAPH Asia)*, 34(6):248:1–248:16, 2015.
- [32] E. Marchand, H. Uchiyama, and F. Spindler. Pose estimation for augmented reality: A hands-on survey. 22(12):2633–2651, 2016. doi: 10.1109/TVCG.2015.2513408
- [33] P. Martinez-Gonzalez, S. Oprea, J. A. Castro-Vargas, A. Garcia-Garcia, S. Orts-Escolano, J. Garcia-Rodriguez, and M. Vincze. UnrealROX+: An improved tool for acquiring synthetic data from virtual 3d environments, 2021.
- [34] Y. Park, V. Lepetit, and W. Woo. Multiple 3d object tracking for augmented reality. In *2008 7th IEEE/ACM International Symposium on Mixed and Augmented Reality*, pp. 117–120. IEEE, 2008.
- [35] K. Pauwels, L. Rubio, J. Diaz, and E. Ros. Real-time model-based rigid object pose estimation and tracking combining dense and sparse visual cues. In *Proceedings of the IEEE conference on computer vision and pattern recognition*, pp. 2347–2354, 2013.
- [36] S. Peng, Y. Liu, Q. Huang, X. Zhou, and H. Bao. Pynet: Pixel-wise voting network for 6dof pose estimation. In *Proceedings of the IEEE/CVF Conference on Computer Vision and Pattern Recognition*, pp. 4561–4570, 2019.
- [37] F. Pomerleau, F. Colas, R. Siegwart, and others. A review of point cloud registration algorithms for mobile robotics. *Foundations and Trends® in Robotics*, 4(1):1–104, 2015.
- [38] V. A. Prisacariu and I. D. Reid. PWP3d: Real-time segmentation

- and tracking of 3d objects. *International journal of Computer Vision*, 98:335–354, 2012.
- [39] W. Qiu and A. Yuille. UnrealCV: Connecting computer vision to unreal engine. In *European Conference on Computer Vision Workshops (ECCVW)*, pp. 909–916, 2016.
- [40] R. Radkowski and J. Ingebrand. HoloLens for Assembly Assistance - A Focus Group Report. In S. Lackey and J. Chen, eds., *Virtual, Augmented and Mixed Reality*, Lecture Notes in Computer Science, pp. 274–282. Springer International Publishing, Cham, 2017. doi: 10.1007/978-3-319-57987-0_22
- [41] J. Rambach, A. Pagani, M. Schneider, O. Artemenko, and D. Stricker. 6dof object tracking based on 3d scans for augmented reality remote live support. 7(1):6, 2018.
- [42] J. Redmon, S. Divvala, R. Girshick, and A. Farhadi. You only look once: Unified, real-time object detection. In *Proceedings of the IEEE conference on computer vision and pattern recognition*, pp. 779–788, 2016.
- [43] S. Rusinkiewicz and M. Levoy. Efficient variants of the ICP algorithm. In *Proceedings third international conference on 3-D digital imaging and modeling*, pp. 145–152. IEEE, 2001.
- [44] H. Schieber, K. C. Demir, C. Kleinbeck, S. H. Yang, and D. Roth. Indoor synthetic data generation: A systematic review. *Computer Vision and Image Understanding*, p. 103907, 2024. doi: 10.1016/j.cviu.2023.103907
- [45] T. Schmidt, R. Newcombe, and D. Fox. Dart: dense articulated real-time tracking with consumer depth cameras. *Autonomous Robots*, 39:239–258, 2015.
- [46] T. J. Schoonbeek, T. Houben, H. Onvlee, P. H. N. de With, and F. van der Sommen. IndustReal: A dataset for procedure step recognition handling execution errors in egocentric videos in an industrial-like setting, 2024.
- [47] A. Stanescu, P. Mohr, M. Kozinski, S. Mori, D. Schmalstieg, and D. Kalkofen. State-aware configuration detection for augmented reality step-by-step tutorials. In *2023 IEEE International Symposium on Mixed and Augmented Reality (ISMAR)*, pp. 157–166. IEEE, 2023.
- [48] M. Stoiber, M. Elsayed, A. E. Reichert, F. Steidle, D. Lee, and R. Triebel. Fusing visual appearance and geometry for multi-modality 6dof object tracking.
- [49] M. Stoiber, M. Pfanne, K. H. Strobl, R. Triebel, and A. Albu-Schäffer. SRT3d: A sparse region-based 3d object tracking approach for the real world. 130(4):1008–1030, 2022.
- [50] M. Stoiber, M. Sundermeyer, W. Boerdijk, and R. Triebel. A multi-body tracking framework—from rigid objects to kinematic structures. 2022.
- [51] M. Stoiber, M. Sundermeyer, and R. Triebel. Iterative Corresponding Geometry: Fusing Region and Depth for Highly Efficient 3D Tracking of Textureless Objects. In *IEEE/CVF Conference on Computer Vision and Pattern Recognition*, 2022.
- [52] Y. Su, M. Liu, J. Rambach, A. Pehrson, A. Berg, and D. Stricker. IKEA object state dataset: A 6dof object pose estimation dataset and benchmark for multi-state assembly objects. 2021.
- [53] Y. Su, J. Rambach, N. Minaskan, P. Lesur, A. Pagani, and D. Stricker. Deep multi-state object pose estimation for augmented reality assembly. In *2019 IEEE International Symposium on Mixed and Augmented Reality Adjunct (ISMAR-Adjunct)*, pp. 222–227, 2019. doi: 10.1109/ISMAR-Adjunct.2019.00-42
- [54] B. Tekin, S. N. Sinha, and P. Fua. Real-time seamless single shot 6d object pose prediction. In *Proceedings of the IEEE Conference on Computer Vision and Pattern Recognition (CVPR)*, 2018.
- [55] H. Tjaden, U. Schwanecke, E. Schömer, and D. Cremers. A region-based gauss-newton approach to real-time monocular multiple object tracking. *IEEE transactions on pattern analysis and machine intelligence*, 41(8):1797–1812, 2018.
- [56] B. Wang, G. Wang, A. Sharf, Y. Li, F. Zhong, X. Qin, D. CohenOr, and B. Chen. Active assembly guidance with online video parsing. In *2018 IEEE Conference on Virtual Reality and 3D User Interfaces (VR)*, pp. 459–466. IEEE, 2018.
- [57] C. Wang, D. Xu, Y. Zhu, R. Martín-Martín, C. Lu, L. Fei-Fei, and S. Savarese. Densefusion: 6d object pose estimation by iterative dense fusion. In *Proceedings of the IEEE/CVF conference on computer vision and pattern recognition*, pp. 3343–3352.
- [58] G. Wang, F. Manhardt, F. Tombari, and X. Ji. Gdr-net: Geometry-guided direct regression network for monocular 6d object pose estimation. In *Proceedings of the IEEE/CVF Conference on Computer Vision and Pattern Recognition*, pp. 16611–16621, 2021.
- [59] H. Wang, S. Sridhar, J. Huang, J. Valentin, S. Song, and L. J. Guibas. Normalized object coordinate space for category-level 6d object pose and size estimation. In *The IEEE Conference on Computer Vision and Pattern Recognition (CVPR)*, 2019.
- [60] R. Wang, Y. Zhang, J. Mao, R. Zhang, C.-Y. Cheng, and J. Wu. Ikea-manual: Seeing shape assembly step by step. In S. Koyejo, S. Mohamed, A. Agarwal, D. Belgrave, K. Cho, and A. Oh, eds., *Advances in Neural Information Processing Systems*, vol. 35, pp. 28428–28440. Curran Associates, Inc., 2022.
- [61] R. Wang, Y. Zhang, J. Mao, R. Zhang, C.-Y. Cheng, and J. Wu. Ikea-manual: Seeing shape assembly step by step. *Advances in Neural Information Processing Systems*, 35:28428–28440, 2022.
- [62] L.-C. Wu, I.-C. Lin, and M.-H. Tsai. Augmented reality instruction for object assembly based on markerless tracking. In *Proceedings of the 20th ACM SIGGRAPH Symposium on Interactive 3D Graphics and Games, I3D '16*, pp. 95–102. Association for Computing Machinery, 2016. doi: 10.1145/2856400.2856416
- [63] P.-C. Wu, Y.-Y. Lee, H.-Y. Tseng, H.-I. Ho, M.-H. Yang, and S.-Y. Chien. A benchmark dataset for 6dof object pose tracking. In *2017 IEEE International Symposium on Mixed and Augmented Reality (ISMAR-Adjunct)*, pp. 186–191. doi: 10.1109/ISMAR-Adjunct.2017.62
- [64] Y. Xiang, T. Schmidt, V. Narayanan, and D. Fox. Posecnn: A convolutional neural network for 6d object pose estimation in cluttered scenes. 2017.
- [65] W. Yan. Augmented reality instructions for construction toys enabled by accurate model registration and realistic object/hand occlusions. *Virtual Reality*, 26(2):465–478, June 2022. doi: 10.1007/s10055-021-00582-7
- [66] M. Zaccaria, F. Manhardt, Y. Di, F. Tombari, J. Aleotti, and M. Giorgini. Self-supervised category-level 6d object pose estimation with optical flow consistency. *IEEE Robotics and Automation Letters*, 8(5):2510–2517, 2023. doi: 10.1109/LRA.2023.3254463
- [67] J. Zauner, M. Haller, A. Brandl, and W. Hartman. Authoring of a mixed reality assembly instructor for hierarchical structures. In *The Second IEEE and ACM International Symposium on Mixed and Augmented Reality, 2003. Proceedings.*, pp. 237–246, 2003. doi: 10.1109/ISMAR.2003.1240707
- [68] H. Zhang, Y. Wang, F. Dayoub, and N. Sunderhauf. Varifocalnet: An iou-aware dense object detector, 2021.